Structural Eng. / Earthquake Eng. Vol. 7. No. 2, 331s-342s. October 1990
Japan Society of Civil Engineers (Proc. of JSCE No. 422/I-14)

AN EMPIRICAL SCALING OF STRONG-MOTION SPECTRA WITH APPLICATION TO ESTIMATE OF SOURCE SPECTRA

By Makoto KAMIYAMA and Tadashi MATSUKAWA***

A new regression model of strong-motion spectra is derived by incorporating the conception of the dummy variables to the conventional regression model. The dummy variables are available not only to obtain the amplification factors due to local soil conditions of each observation site but also to estimate the non-linear dependences of spectral amplitude on earthquake magnitude and hypocentral distance. The new regression model is applied to 228 strong-motion spectra obtained in Japan. The regression results are used to estimate the source spectra, as well as being discussed in detail, in particular, from the view points of faulting and wave propagation mechanisms. It is finally concluded that the specific barrier model is more connected with the present statistical source spectra than the stochastic ω-square model.

Keywords: *strong-motion spectra, statistical analysis, dummy variable, source spectra*

1. INTRODUCTION

In order to estimate strong motions incident to structures, statistical analyses of strong-motion spectra have been performed so far by many researchers throughout the world[1)~3)]. Most of these works were based on the multiple regression technique in terms of simple parameters such as earthquake magnitude, source-to-station distance and so on, even though some additional parameters reflecting the effects due to local site conditions are included or not. As well known, earthquake ground motions are caused by the three principal factors of source, propagation path of waves and local soil layers, so it is necessary to take the effects resulting from these factors into account for the purpose of statistical analyses of strong motions. Above simple parameters such as earthquake magnitude which have been usually employed in engineering field were introduced into statistical analyses as convenient variables for expressing these factors. The source characteristics of earthquake, however, are too complicated to be expressed merely by earthquake magnitude. Similarly, it would be insufficient to represent the complex propagation path of waves only by the source-to-station distance.

There may be several ways to overcome these difficulties, for instance, an effective way would be to introduce more physical parameters based on the faulting source model of earthquake, instead of using convenient variables like earthquake magnitude. Motivated by such idea, one of the authors tried to make a preliminary statistical analysis of strong-motion spectra using the faulting source parameters of seismic moment and fault length[4)]. However, such a kind of statistical analysis has its limit at present because faulting parameters are not known about small earthquakes, although it has a bright future when data will

* Member of JSCE, Dr. Eng. Professor, Dept. of Civil Eng., Tohoku Institute of Technology (Yagiyama-Kasumicho 35, Taihaku-ku, Sendai 982, Japan)
** Member of JSCE, Assistant, Dept. of Civil Eng., Tohoku Institute of Technology

become more abundant. Another way to achieve the above goal is to work on the regression model of statistical analysis, while using the conventional variables of earthquake magnitude and source-to-station distance. Even such simplified variables would make it possible to follow the effects owing to complicated source characteristics and compound propagation path of waves when some skillful ideas were added to the regression model.

As an attempt of the latter way, this paper deals with a new type of regression model of strong-motion spectra and derives an empirical scaling law of spectra by introducing the conception of the dummy variable. The source spectra statistically derived by the model is also examined in comparison with the theoretical source spectra proposed so far.

2. SOME PROBLEMS RELATING TO THE CONVENTIONAL REGRESSION MODELS OF STRONG-MOTION SPECTRA

In analyzing statistically strong-motion data such as spectra, most workers have assumed the following type of regression model to fit the data.

$$\log_{10} V(T)=a(T)M+b(T)\log_{10} r+c(T), \quad \cdots\cdots (1)$$

where $V(T)$: strong-motion spectra, M : earthquake magnitude, r : epicentral distance or hypocentral distance, $a(T)$, $b(T)$ and $c(T)$: regression coefficients, and T : period.

Although the reason leading to Eq. (1) is rather unclear, the definition of earthquake magnitude proposed by Richter[5] may be used in it, namely, the expression of defining earthquake magnitude by Richter can produce Eq. (1) by replacing the maximum amplitude of displacement with the spectral amplitudes.

Eq. (1) includes several unfavorable problems for following actual strong-motion data whereas it is useful in engineering practice because of its simplicity. The first problem is that it is not due to physical mechanism of earthquake, and therefore it may give little reliability when being applied beyond its original data band. The second is that Eq. (1) is a kind of linear model against the variables M and r, that is, it takes a prior assumption that the dependence of the objective variable $V(T)$ on the explanatory variables M and r is constant irrespective of their amplitudes, as shown schematically in Fig. 1. And, the third is that measuring of r needs careful consideration, especially, when faults of large earthquakes are in question. Among the above problems, Takemura *et al.*[6] discussed the first problem theoretically from a view point of earthquake fault model and provided a little different regression expression in terms of seismic moment. Even though their regression analysis is based on a physical understanding, it is a kind of linear expression because of the derivation limited to a uniform fault model. On the other hand, the second problem may be particularly important from engineering standpoint because it directly controls the scaling law of spectra. In addition, there is a possibility to overcome the first and third problems by resolving the second one, considering that the complexities of earthquake mechanism and propagation manner of waves would result in some non-linear relationships between strong motions and earthquake parameters. In this paper we

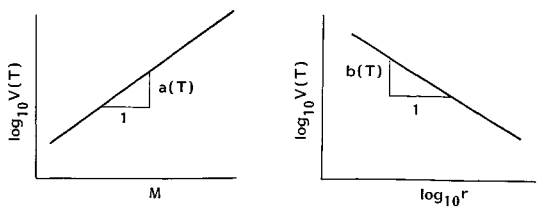

Fig. 1 Schematic diagram for the dependence of the objective variable on the explanatory variables in the conventional regression model.

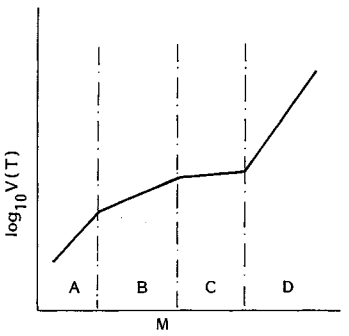

Fig. 2 Conception of the present regression model.

mainly discuss a method of attacking the second problem.

One of the easiest method to reach a goal for the problem is to reform the coefficients $a(T)$ and $b(T)$ in Eq. (1) so that they depend on the variables M and $\log_{10} r$, as follows.

$$a(T)=a'(T)M+a''(T)\log_{10} r+\cdots\cdots, \quad (2)$$

$$b(T)=b'(T)M+b''(T)\log_{10} r+\cdots\cdots. \quad (3)$$

Such a method means to introduce higher power terms of explanatory variables into the regression model, as being seen by substituting Eqs. (2) and (3) into Eq. (1). Therefore we can construct unlimitedly complex regression models by use of such ideas, in particular, by using power terms as high as possible. This idea has been already employed for the statistical analyses of strong motions by several researchers[7]. The authors also made statistical analysis of strong-motion spectra on the basis of the regression model of power terms[8]. Even though this method is effective to some extent to follow rather complicated variation of the objective variable, its main drawback is that it restricts the variation by its specific functional form.

Another method different from the above is to join several linear functions together so as to follow the complicated variation. The conception of the method is schematically shown in Fig. 2, as an example of one explanatory variable M. This method stipulates for a linear variation in each local region of the variable, but it has an advantage to simulate appropriately the overall non-linear variation of variables. In addition to such an advantage, the method can not only make clear some points where the objective variable begins to vary remarkably in accordance with the explanatory one, but also fit efficiently to data whose numbers are uneven in their each region. The problem peculiar to the method, however, is how to determine the transition points and gradients of each linear function. Such determinations are explained in the following section.

3. MULTIPLE REGRESSION MODEL USING THE DUMMY VARIABLES

(1) Idea of the present regression model

In an attempt to make the explanation clear, we first confine ourselves to the simplest case provided with one objective variable $V(T)$ and one explanatory variable M which are assumed to be spectral amplitude and earthquake magnitude, respectively. The scatter diagram of the case is modeled in Fig. 3. This may be fitted by several combinations of various linear functions, but the simplest combination of two linear functions would be enough to explain the principle for fitting. So we explain the method for determining the boundary point and gradients of the two linear functions using the model in Fig. 3.

Now suppose that the data were divided into two groups by setting an arbitrary value M_c, as shown in Fig. 3. Then we build the following regression model in which the conception of the dummy variable is included.

$$\log_{10} V(T)=a_1(T)M_1+a_2(T)M_2+a_3(T)M_3+a_4(T), \quad (4)$$

where the explanatory variables M_1, M_2 and M_3 are given as

$$M_1=\begin{cases} M & (M\leqq M_c) \\ M_c & (M>M_c) \end{cases}, \quad M_2=\begin{cases} 0 & (M\leqq M_c) \\ M-M_c & (M>M_c) \end{cases}, \quad M_3=\begin{cases} 0 & (M\leqq M_c) \\ 1 & (M>M_c) \end{cases},$$

and $a_1(T)$, $a_2(T)$, $a_3(T)$ and $a_4(T)$ are regression coefficients in which $a_3(T)$ has minus sign in the case of Fig. 3.

By applying the least square technique to Eq. (4), we can estimate the coefficients $a_1(T)$, $a_2(T)$, $a_3(T)$ and $a_4(T)$, and then the target value M_0 is obtained, as follows, using these coefficients.

$$M_0=M_c+a_3(T)/(a_1(T)-a_2(T)). \quad (5)$$

The relations between these coefficients and the boundary value M_0 are indicated in Fig. 3. After one boundary value M_0 was obtained as stated above, we retry the regression analysis by using the value as a new value of M_c. Thus we finally can obtain the most suitable regression model of two linear functions when such iteration leads to some convergent regression coefficients. Fig. 3 is an example of the conjunction of two linear functions for two variables, but it is easily extended to more multiple linear functions as well as

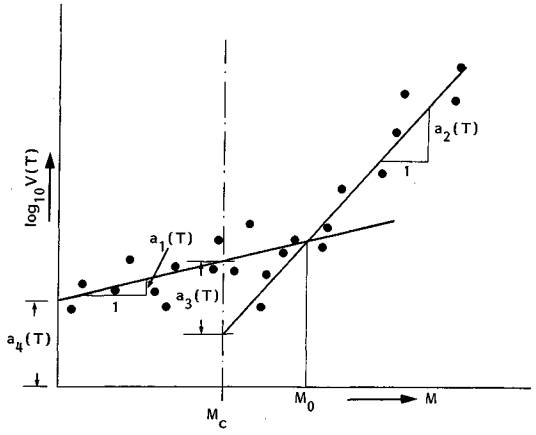

Fig. 3 A model of scatter diagram of data where $V(T)$ and M mean, respectively, spectral amplitude and earthquake magnitude. The model is fitted by the combination of two linear functions.

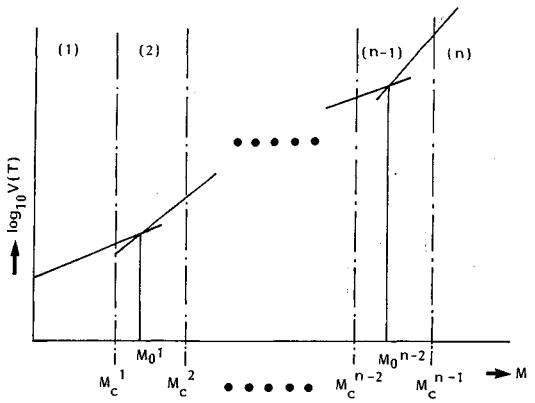

Fig. 4 Model of multiple linear functions for the regression analysis.

more numerous variables. Referring to Fig. 4, for instance, the regression model consisting of n linear functions for one explanatory variable M is written as

$$\log_{10} V(T)=\sum_{i=1}^{2n-1} a_i(T)M_i+a_{2n}(T), \quad \cdots\cdots (6)$$

where we give the variables M_i in the following manner.

$$M_1=\begin{cases} M & (M\leqq M_c^1) \\ M_c^1 & (M>M_c^1) \end{cases}, \quad M_i=\begin{cases} 0 & (M\leqq M_c^{i-1}) \\ M-M_c^{i-1} & (M_c^{i-1}<M\leqq M_c^i) \\ M_c^i-M_c^{i-1} & (M>M_c^i) \end{cases} \quad (i=2\sim n-1),$$

$$M_n=\begin{cases} 0 & (M\leqq M_c^{n-1}) \\ M-M_c^{n-1} & (M>M_c^{n-1}) \end{cases}, \quad M_{n+i}=\begin{cases} 0 & (M\leqq M_c^i) \\ 1 & (M>M_c^i) \end{cases} \quad (i=1\sim n-1),$$

in which M_c^i $(i=1\sim n-1)$ are preliminary boundary values for classifying M. The target boundary values M_0^i $(i=1, 2, \cdots, n-2)$ are given by the same manner as Eq. (5). This method is hereafter called "dummy variable regression" in short.

(2) Regression model used in the present study

It may depend principally on the number of the used data and their physical background how many linear functions should be built in the above type of regression analysis. In our regression analysis of strong-motion spectra, on the other hand, we use earthquake magnitude M and hypocentral distance r as the explanatory variables for the objective variable of spectral amplitude $V(T)$ according to Eq. (1). Furthermore, we add other explanatory variables for estimating the amplification factors due to local site conditions of each observation site. That is, on the condition that the observation sites are N in total, we use the model

$$\log_{10} V(T)=a(T)M+b(T)\log_{10} r+c(T)+\sum_{j=1}^{N-1} A_j(T)S_j, \quad \cdots\cdots (7)$$

where $A_j(T)$ are regression coefficients for S_j.

In Eq. (7), S_j $(j=1, 2, \cdots, N-1)$ are the additional explanatory variables which are treated by the conception of the dummy variables as well as M_3 in Eq. (4). The treatment of S_j was fully explained in our previous paper[9] and it was also shown in the paper that the introduction of such variables is quite fruitful to estimate the local site effects of each observation site. Next we apply the "dummy variable regression" to both of the explanatory variables M and r in Eq. (7). The selection of the number of linear functions applied to both variables is important to derive some detailed scaling of strong-motion spectra, but in order

to obtain reasonable scaling, it is restricted by the physical background causing strong motions, the number of data, the requirement from practical use and so on. We here determined the number of linear functions for both variables in the following consideration.

The attenuation characteristics of earthquake ground motions may result from various factors, for example, source fault behavior, geometrical spreading due to body waves and surface waves, and inelastic effects of propagation media. Of these factors, the fault behavior exerts an influence on the area relatively close to the source, and the second and third factors have greater effects on the area far from the source. As for the distant area from the source, moreover, it would be distinguished by two parts which are exclusively affected by body waves or surface waves, respectively. Thus the attenuation manner of earthquake motions according to hypocentral distance r may be divided into three parts. Meanwhile, there seems to be no clear criteria for classifying earthquake magnitude M based on the physical consideration. We here classify earthquake magnitude M into three parts in a similar way to hypocentral distance, partly making reference to the Japanese Meteorological Agency criteria for earthquake magnitude in which earthquakes of magnitudes greater than or equal to 7 are called the "large earthquake", ones of $7>M\geqq5$ called the "intermediate earthquake", and ones of $5>M\geqq3$ called the "small earthquake". In reference to the above consideration, we divide both variables of M and r into three parts and we finally build the following regression model.

$$\log_{10} V(T)=\sum_{i=1}^{5} a_i(T)M_i+\sum_{i=1}^{5} b_i(T)R_i+c(T)+\sum_{j=1}^{N-1} A_j(T)S_j, \quad \cdots\cdots (8)$$

where

$$M_1=\begin{cases} M & (M\leqq M_c^1) \\ M_c^1 & (M>M_c^1) \end{cases}, \quad M_2=\begin{cases} 0 & (M\leqq M_c^1) \\ M-M_c^1 & (M_c^1<M\leqq M_c^2) \\ M_c^2-M_c^1 & (M>M_c^2) \end{cases}, \quad M_3=\begin{cases} 0 & (M\leqq M_c^2) \\ M-M_c^2 & (M>M_c^2) \end{cases},$$

$$M_4=\begin{cases} 0 & (M\leqq M_c^1) \\ 1 & (M>M_c^1) \end{cases}, \quad M_5=\begin{cases} 0 & (M\leqq M_c^2) \\ 1 & (M>M_c^2) \end{cases},$$

$$R_1=\begin{cases} \log_{10} r & (r\leqq r_c^1) \\ \log_{10} r_c^1 & (r>r_c^1) \end{cases}, \quad R_2=\begin{cases} 0 & (r\leqq r_c^1) \\ \log_{10} r-\log_{10} r_c^1 & (r_c^1<r\leqq r_c^2) \\ \log_{10} r_c^2-\log_{10} r_c^1 & (r>r_c^2) \end{cases},$$

$$R_3=\begin{cases} 0 & (r\leqq r_c^2) \\ \log_{10} r-\log_{10} r_c^2 & (r>r_c^2) \end{cases}, \quad R_4=\begin{cases} 0 & (r\leqq r_c^1) \\ 1 & (r>r_c^1) \end{cases}, \quad R_5=\begin{cases} 0 & (r\leqq r_c^2) \\ 1 & (r>r_c^2) \end{cases}.$$

4. REGRESSION ANALYSIS FOR STRONG-MOTION SPECTRA OBTAINED IN JAPAN

(1) Conditions for the regression analysis

The regression model of Eq. (8) was applied to the strong-motion records observed in Japan. The data are the same as the ones in the study of Ref. 9), that is, they consist of 228 horizontal accelerograms of maximum amplitude greater than 20 gal. The earthquake origins for these accelerograms are shown in Fig. 5 together with the total observation sites of 26. These accelerograms were observed on the conditions of JMA magnitudes ranging from 4.1 to 7.9, focal depths from 0 to 130 km, and epicentral distances from 3 to 350 km.

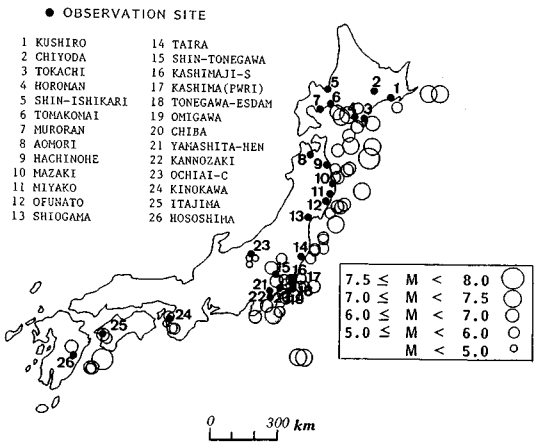

Fig. 5 Map of the earthquake origions and observation sites for the strong-motion records.

The earthquake magnitude, focal depth and epicentral distance peculiar to each accelerogram are shown in Table 1 of Ref. 9). We computed velocity response spectra with no damping from these strong-motion accelerograms and applied them to $V(T)$ in Eq. (8). The main reason for using velocity response spectra with no damping is that they are nearly equivalent to Fourier acceleration spectra, which are most suited for the discussion of source spectra, even though they are easy to compute.

In Eq. (8), we are required to allot one site among all the observation sites to a reference site by which the amplification factors specific to each site can be estimated with enough physical implication. We here adopted Ofunato site labelled 12 in Fig. 5 as the reference site for the same reason described in Ref. 8). That is, Ofunato site consists of the hardest rock among all the observation sites and is rigid enough to constitute the bed rock for the other sites. The outcrop of the site is a hard slate whose S wave velocity is supposed to be 1~2 km/sec. Accordingly the "bed rock" implied in this paper is a rock having such a rigidity.

About the initial boundary values M_c^1, M_c^2, r_c^1 and r_c^2 in Eq. (8), meanwhile, we employed tentatively as $M_c^1=5.5$, $M_c^2=7.0$, $r_c^1=30$ km and $r_c^2=100$ km considering the distribution of the data, and then almost convergent regression coefficients were gained after three iterations of analysis. The regression coefficients given in the following are the results based on the three iterations of analysis.

(2) Results of the regression analysis

We carried out the regression analysis of Eq. (8) using the above data and conditions, and compared the results with that of the regression model for Ref. 9). The correlation coefficients obtained by Eq. (8) were found to become better for all the periods in comparison with the correlation results of Ref. 9), for example, showing a change of the multiple correlation coefficient and standard deviation, respectively, from 0.81 to 0.87 and from 0.26 to 0.25 for the period of 1.0 sec. In the following, the analyzed results are shown for each regression coefficient.

First we show the results of the coefficients $A_j(T)$ in Eq. (8) which are given by $2\cdot10^{A_j(T)}$ so as to express amplification factors of each site against the bed rock. Fig. 6 is the amplification factors determined for representative observation sites as a function of period. It is seen in Fig. 6 that the amplification factors are quite peculiar to each site and are strongly period-dependent. The amplification factors shown in Fig. 6 are almost the same as the ones which were obtained from the regression models of Refs. 8) and 9) different from the present model in treating earthquake factors. This means that such regression model as Eq. (8) is efficient to make clear the effects due to local site conditions since amplification factors are similarly obtained irrespective of the treatments of earthquake factors.

The results of the regression coefficients $a_1(T)$, $a_2(T)$ and $a_3(T)$ in Eq. (8) are shown in Fig. 7 as a period function. As shown in Fig. 7, these coefficients stand for the gradients of each linear function with regard to the explanatory variable M. On the other hand, the transition values M_0^1 and M_0^2 of the linear functions which were obtained from the coefficients $a_1(T)$~$a_5(T)$ are plotted in Fig. 8. We can see from

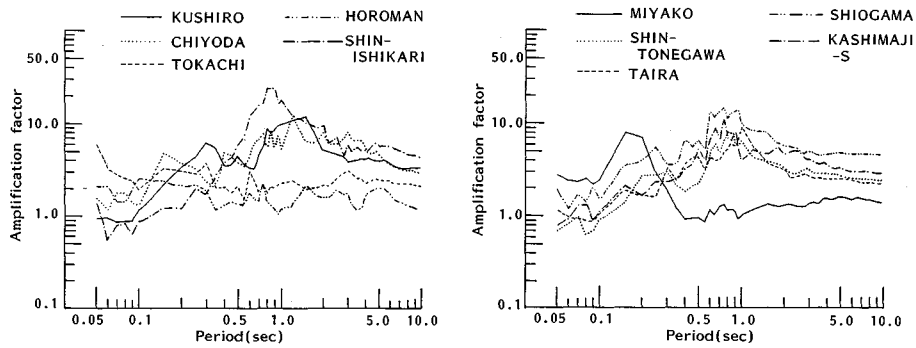

Fig. 6 Amplification factors at the representative observation sites estimated from the regression analysis.

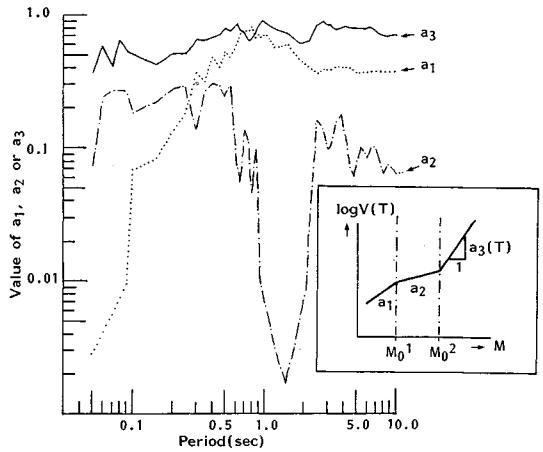

Fig. 7 Regression coefficients $a_1(T)$, $a_2(T)$ and $a_3(T)$ of earthquake magnitude M obtained from the least square analysis.

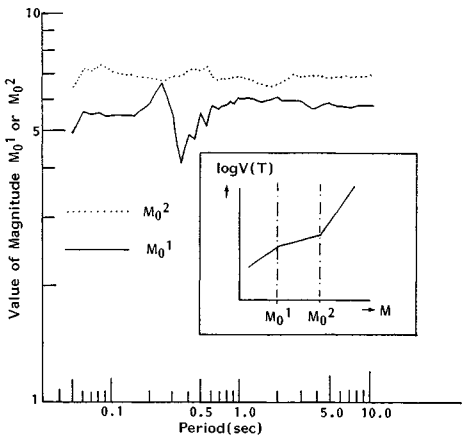

Fig. 8 Transition values M_0^1 and M_0^2 of the linear functions with regard to earthquake magnitude M estimated from the regression analysis as a function of period.

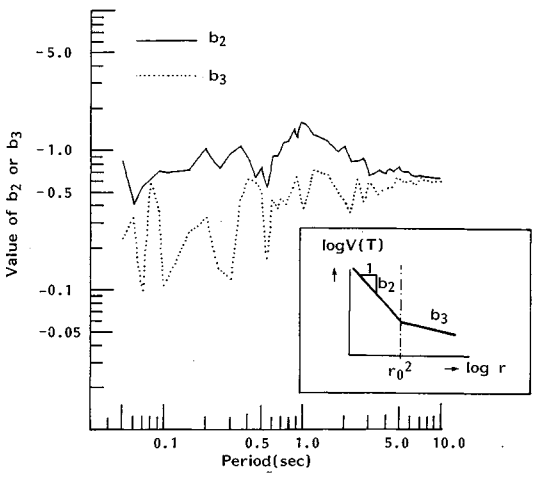

Fig. 9 Regression coefficients $b_2(T)$ and $b_3(T)$ with regard to hypocentral distance r obtained from the least square analysis.

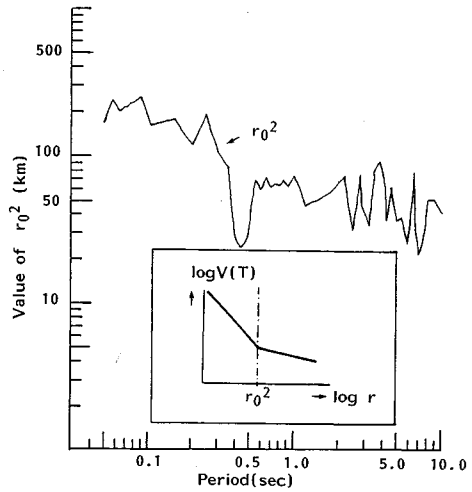

Fig. 10 Transition value r_0^2 with regard to hypocentral distance r estimated from the regression analysis as a function of period.

Figs. 7 and 8 that the dependence of $V(T)$ on M varies remarkably relying on the absolute value of M as well as on period. For instance, the dependency is greater in all the periods for larger magnitudes than about 7.0 and it is conversely smaller for magnitudes less than 7.0, particularly, in both regions of the periods greater than about 0.5 sec for the magnitudes from about 5 to 7 and of the periods shorter than about 0.5 sec for the magnitudes less than about 5.0. These results show that spectral amplitude of earthquake motions responds complicatedly to the variation of magnitude M being different from the conventional simple regression models. This may reflect the difference in faulting mechanism of earthquake varied according to earthquake magnitude. At least Figs. 7 and 8 suggest that there is a marked difference in earthquake faulting mechanism between below and above around $M=6.5$.

Next the regression coefficients $b_1(T)$, $b_2(T)$ and $b_3(T)$ and the transition values of hypocentral distance r are shown in Figs. 9 and 10. In this case, the transition value r_0^1 became asympotic almost to zero in all

the periods after the three iterated regression analyses, so only the coefficients $b_2(T)$, $b_3(T)$ and the second transition value r_0^2 are given in Figs. 9 and 10. As described in the preceding section, the coefficients $b_2(T)$ and $b_3(T)$ mean the attenuation characteristics of earthquake motions which include geometrical spreading due to body waves and surface waves, inelastic effects of propagation media and so on. It is seen in Figs. 9 and 10 that the attenuation is stronger in the areas less than r_0^2 in all the periods even though it fluctuates depending on period, and that the transition value r_0^2 has a general tendency to increase with decreasing period. In order to compare the attenuation characteristics in accordance with hypocentral distance r, Fig. 11 was produced from Figs. 9 and 10 so that the coefficients $b(T)$ of $\log_{10} r$ are plotted at the three representative distances. As well known, the attenuations caused by the spreading distance r are r^{-1} and $r^{-0.5}$, respectively, for body waves and surface waves. Although strong period-dependence is visible, it seems that the coefficient $b(T)$ in Fig. 11 is generally consistent with the geometrical spreading due to body waves and surface waves, indicating that prominences of both sorts of waves vary in response to distance and period. It may be suggested from the values of $b(T)$ in Fig. 11 that body waves are mainly predominant in the periods shorter than around 3 sec at the distance r equal to 50 km while surface waves dominate in all the periods at $r=150$ km, and at $r=80$ km there is a cross-over period of about 0.5 sec above and below which surface waves and body waves each prevail.

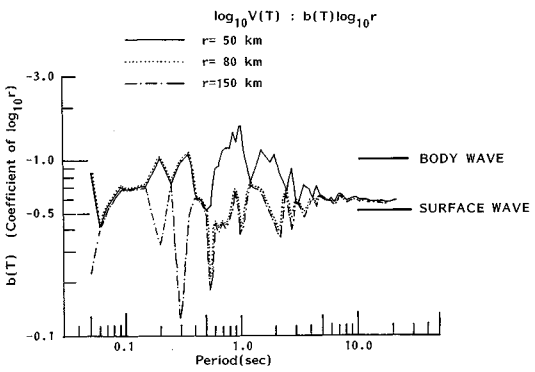

Fig. 11 Attenuation coefficients $b(T)$ due to hypocentral distance r derived from the regression analysis. The hypocentral distance r is set to be 50, 80 and 150 km.

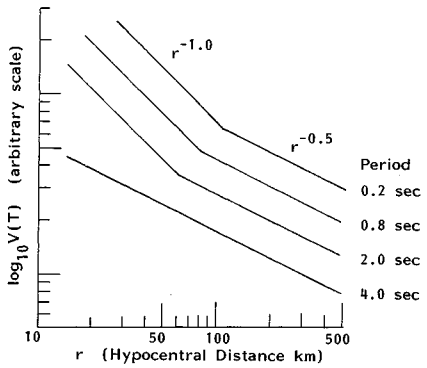

Fig. 12 A model diagram for the attenuation of spectral amplitude according to hypocentral distance r and period T. The vertical axis is taken as a arbitrary scale of $\log_{10} V(T)$ where $V(T)$ means spectral amplitude. The attenuation manners r^{-1} and $r^{-0.5}$ correspond each to body waves and surface waves.

Disregarding the fine fluctuation of $b(T)$ with period T, we constructed a model diagram of attenuation which was drawn by emphasizing the general trend of $b(T)$, as shown in Fig. 12. Fig. 12 reveals that there would exist a cross-over distance ranging from about 50 km to 100 km over which dominant waves change from body waves to surface waves, and the cross-over distance is dependent on period so that it becomes greater with shorter period. Although the effect due to focal depth was not considered in the above discussion, the attenuation manner shown in Fig. 12 would be acceptable in reference to our previous study[9] in which the explanatory variable of focal depth was already found to exert little practical effect on spectral amplitudes.

5. SCALING OF STRONG-MOTION SPECTRA INCLUDING SOURCE SPECTRA

Using the regression coefficients stated above, we can scale strong-motion spectra in terms of earthquake magnitude M, hypocentral distance r and local site effects. In this paper we focus our attention on the spectra only due to M and r in consideration of their characteristic coefficients obtained in the above section. Such spectra are here referred to as "rock site spectra" since they are not covered by

the effects owing to local soil layers.

Fig. 13 shows an example of rock site spectra scaled with M while keeping r equal to 80 km which is the averaged hypocentral distance in the original strong-motion data. The spectra were estimated according to Eq. (8) except for the last summation term in the right side. It is clear in Fig. 13 that each spectrum tends to have nearly flat configurations between two corner periods although long-period components become more predominant relative to short-period ones with increasing magnitude M. The overall scaling manner of spectra in Fig. 13 is comparatively similar to that based on the regression model in Ref. 8), but it is emphasized in Fig. 13 that spectral amplitudes have less variation between $M=6.0$ and $M=6.5$. Anyway, the scaling manner of spectra obtained here is relatively compatible to the strong-motion spectra observed in the Guerrero's rock site array[10] in the point of how the dependence of spectral amplitudes on earthquake magnitude varies according to periods.

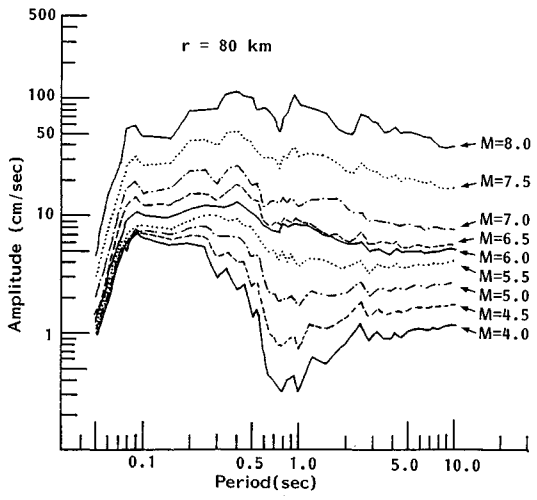

Fig. 13 Rock site spectra statistically scaled with earthquake magnitude M while keeping hypocentral distance r equal to 80 km.

As a significant contribution, on the other hand, such rock site spectra as Fig. 13 make it possible to estimate the so-called source spectra. Since Gusev's discussion[11], the source spectra of acceleration motions have been investigated by several workers on account of their importance from engineering standpoint, particularly, there has been a hot debate between the two schools of the "stochastic ω-square model" by Hanks and McGuire[12] and the "specific barrier model" by Papageorgiou and Aki[13] over their validities. We here discuss the source spectra of acceleration motions by use of the statistically scaled rock site spectra.

Gusev[11] defined the source spectra of acceleration motions as $f^2\cdot\tilde{\dot{M}}_0(f)$, where f and M_0 are, respectively, frequency and seismic moment, and $\cdot$ and $\sim$ mean each time derivative and Fourier transform, because it is equivalent theoretically to acceleration spectra only due to source parameters. As shown by Papageorgiou[14], such source spectra can be derived in the following form on the condition that acceleration motion spectra $u(f, r)$ caused by body waves are available at a hypocentral distance r on a homogeneous half space where the source exists.

$$f^2\cdot\tilde{\dot{M}}_0(f)=\frac{4\pi\rho\beta^3 r}{F_s}\frac{1}{(2\pi)^2}\frac{\sqrt{2}}{2}u(f, r), \quad \cdots\cdots (9)$$

where β : shear wave velocity, ρ : density of the space and F_s : radiation pattern coefficient peculiar to the shear dislocation.

In our case, the rock site spectra like Fig. 13 would be regarded as $u(f, r)$ on the assumption that the "bed rock" described in the preceding section is equivalent to the homogeneous half space of Eq. (9). Such assumption may be rather rough judging from the rigidity of the bed rock whose S wave velocity is supposed to be 1~2 km/sec, as shown above. However, our rock site spectra would be used as a replacement of $u(f, r)$ if being allowed to assume that an inelastic effect of the half space disregarded in Eq. (9) is almost equal to an amplification effect between our bed rock and the half space.

When using Eq. (9) to estimate the source spectra, meanwhile, a careful selection of r is needed because it results from only body waves, namely, we need $u(f, r)$ and r related only to body waves. In this point, the present regression model is useful to confirm whether or not to result from body waves. As

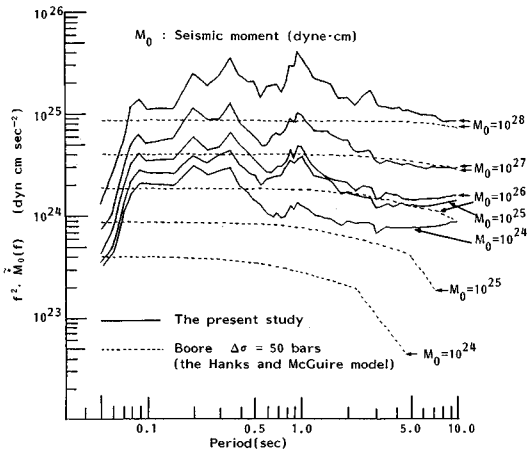

Fig. 14 Comparison between the theoretical source spectra due to the "stochastic ω-square model" by Hanks and McGuire and the present statistical source spectra. The theoretical source spectra were estimated using the parameters given by Boore[16].

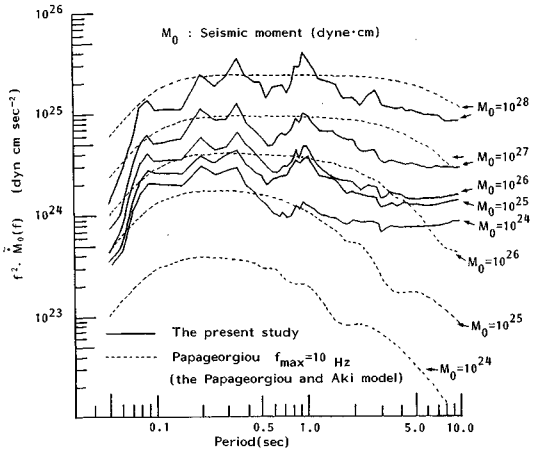

Fig. 15 Comparison between the theoretical source spectra due to the "specific barrier model" by Papageorgiou and Aki and the present statistical source spectra. The theoretical source spectra were estimated using the parameters given by Papageorgiou[14].

explained previously, the rock site spectra within the periods shorter than about 3.0 sec estimated at r less than 50 km according to Eq. (8) are due primarily to body waves rather than surface waves. In reference to this, we obtained $u(f, r)$ as the rock site spectra at $r=30$ km which is roughly intermediate distance within the body waves zone. The other constants in Eq. (9) were set to be the same as the ones employed in Ref. 8), that is, $\beta=3.5$ km/sec and $F_s=0.63$ for the same reason in the reference. In addition, $\rho=3.0$ g/cm^3 was alloted in consideration of the averaged values of density of the crust arround Japan.

By using the above constants and $u(f, r)$, we can estimate the source spectra $f^2 \cdot \tilde{M}_0(f)$ according to Eq. (9). These spectra may be called statistical source spectra because they are obtained based on the statistical analyses. Different from such statistical method, the source spectra $f^2 \cdot \tilde{M}_0(f)$ can be derived from several faulting source models which are represented by the two schools stated above. Here the statistical spectra are compared to the theoretical spectra due to both models in order to examine each model's validity. Fig. 14 and Fig. 15 show, respectively, the comparisons of the present statistical spectra against the "stochastic ω-square model" (called the HM model hereafter) and the "specific barrier model" (the PA model). In both figures, the statistical spectra are scaled with seismic moment M_0 instead of earthquake magnitude M by using the M_0-M relations by Sato[15]

$$\log M_0 = 1.5\,M + 16.2. \quad \cdots\cdots (10)$$

Also the parameters of the HM model and the PA model in the figures were borrowed, respectively, from Boore[16] and Papageorgiou[14]. It is found in Fig. 14 that there is a remarkable difference between the HM model and the statistical spectra, particularly, the spectral amplitudes due to the model are much smaller than the statistical in shorter periods, although there seems to be the same level spectral amplitude in longer periods for seismic moment M_0 greater than 10^{26}. This may be caused by the reason that the HM model includes hardly the proper heterogenuity of stress drop responsible for high-frequency motion generation. In contrast to the difference, we can find a relatively good agreement between the PA model and the statistical spectra in Fig. 15 except for seismic moments less than 10^{25}. Judging from the comparisons shown in Figs. 14 and 15, it would be concluded that the specific barrier model, which contains both of the local stress drop pertinent to the generation of high-frequency motions and the global stress drop over the entire fault plane for low-frequency motions, is more suitable to estimate the spectral

amplitudes for the large-earthquakes and short-periods which are primarily in question in engineering analyses. Similar conclusion was also derived from our another study[4] which analyzed statistically strong-motion spectra by using fault parameters.

Despite the above conclusion, it remains unsolved how we consider the difference between the statistical and both models for small-earthquakes less than $M_0=10^{25}$. As for this difference there may be several causes possibly coming from both of the models and the statistical results. For example, the fact that the number of small-earthquakes constituting the present data is fewer in intermediate and long distances may lead to the difference. Anyway, the discussion about such causes requires many pages, so in this paper we confine ourselves to the above conclusion with regard to the large-earthquakes.

6. CONCLUDING REMARKS

In this paper, a regression analysis of strong-motion spectra was carried out by using the dummy variables. The dummy variables were used not only to obtain the amplification factors due to local soil conditions of each observation site but also to estimate non-linear dependence of the spectral amplitude on earthquake magnitude M and hypocentral distance r. In addition to being discussed in detail, the results of regression analysis were applied to the estimate of the source spectra. The principal remarks concluded from this study are :

(1) The introduction of the dummy variables to regression analysis of strong motion data is quite effective for raising the reasonability of analysis. The variables make clear the site effects specific to each observation site as amplification factors, and at the same time they provide reasonable variations of strong-motion spectra with M and r.

(2) The dependence of strong-motion spectra on M showed remarkable non-linearity depending on period. In particular, there is a big difference in the dependence between above and below around $M=6.5$. This suggests that earthquake faulting mechanism differs in both bands of earthquake magnitude.

(3) The attenuation of strong-motion spectra according to hypocentral distance r also indicated non-linear characteristics corresponding to the geometrical spreading of body waves and surface waves. There is a cross-over distance ranging from about 50 km to 100 km below and above which body waves and surface waves prevail, respectively, and the distance is so period-dependent that it increases as period becomes shorter.

(4) The source spectra were empirically scaled by use of the regression analysis of spectra. We compared the empirical source spectra with the theoretical ones due to the two stochastic source models, and it was shown from the comparisons that the specific barrier model is more appropriate to estimate the spectral amplitudes for the large-earthquakes and short-periods than the stochastic ω-square model.

On account of space consideration, it has not been discussed in this paper how the present results are related to other types of regression analyses, for example, the analysis by Katayama *et al.*[2] who employed the so-called quantification method. Katayama *et al.* examined indirectly the non-linear dependence of spectral amplitude on M and r through the quantification method, so it is of interest how their results are related to the present study. In addition, the variations of the regression coefficients shown in Figs. 7 to 10 may reflect some physical phenomena of earthquake faulting and propagation manner of waves, and it is also of interest how they are explained quantitatively by sophisticated physical models of earthquake. These interests will be handled in our another paper.

REFERENCES

1) Trifunac, M. D. : Preliminary empirical model for scaling Fourier spectra of strong ground acceleration in terms of earthquake magnitude, source-to-station distance, and recording site conditions, Bull. Seism. Soc. Am. Vol. 66, pp. 1343-1373, 1976.

2) Katayama, T., Iwasaki, T. and Saeki, M. : Statistical analysis of earthquake acceleration response spectra, Proc. of JSCE,

No. 275, pp. 29-40, 1978 (in Japanese).
3) Kobayashi, H. and Nagahashi, S. : Characteristics of earthquake motion on seismic bedrock, Proc. 3rd Japan Earthq. Eng. Symp., pp. 209-216, 1975 (in Japanese).
4) Kamiyama, M. : Regression analyses of strong-motion spectra in terms of a simplified faulting source model, Proc. of 4th World Conference on Soil Dynamics and Earthq. Eng., Vol. 1, pp. 113-126, 1989.
5) Richter, C. F. : An instrumental magnitude scale, Bull. Seism. Soc. Am., Vol. 25, pp. 1-32, 1935.
6) Takemura, M., Ohta, T. and Hiehata, S. : Theoretical basis of empirical relations about response spectra of strong ground-motions, Trans. of the Arch. Inst. of Japan, No. 375, pp. 1-9, 1987 (in Japanese).
7) McGuire, R. K. : A simple model for estimating Fourier amplitude spectra of horizontal ground acceleration, Bull. Seism. Soc. Am., Vol. 68, pp. 803-822, 1978.
8) Kamiyama, M. : Earthquake source characteristics inferred from the statistically analyzed spectra of strong motions with aid of dynamic model of faulting, Structural Eng. and Earthq. Eng., Vol. 4, No. 2, pp. 391-400, 1987.
9) Kamiyama, M. and Yanagisawa, E. : A statistical model for estimating response spectra of strong earthquake motions with emphasis on local soil conditions, Soils and Foundations, Vol. 26, No. 2, pp. 16-32, 1986.
10) Anderson, J. G. and Quaas, R. : Gurrero, Mexico strong array, Proc. of 9th World Conference on Earthq. Eng., Vol. 8, pp. 143-149, 1988.
11) Gusev, A. A. : Descriptive statistical model of earthquake source radiation and its application to an estimation of short-period strong motion, Geophs. J. R. Astr. Soc., Vol. 74, pp. 787-808, 1983.
12) Hanks, T. C. and McGuire, R. K. : The character of high-frequency strong ground motion, Bull. Seism. Soc. Am., Vol. 71, pp. 2071-2098, 1981.
13) Papageorgiou, A. S. and Aki, K. : A specific barrier model for the quantitative description of inhomogeneous faulting and the prediction of strong ground motion, Part 1 and Part 2, Bull. Seism. Soc. Am., Vol. 73, pp. 693-722, pp. 953-978, 1983.
14) Papageorgiou, A. S. : On two characteristic frequencies of acceleration spectra : patch corner frequency and f_{max}, Bull. Seism. Soc. Am., Vol. 78, pp. 509-529, 1988.
15) Sato, R. : Theoretical basis on relationships between focal parameters and earthquake magnitude, J. Phys. Earth., Vol. 27, pp. 353-372, 1979.
16) Boore, D. M. : Short-period P and S-wave radiation from large earthquake : implication for spectral scaling relations, Bull. Seism. Soc. Am., Vol. 76, pp. 43-64, 1986.

(Received October 11 1989)